Available online at www.sciencedirect.com
SCIENCE DIRECT®
Journal of Nuclear Materials 329–333 (2004) 74–80
journal of nuclear materials
www.elsevier.com/locate/jnucmat

# Major results of the cooperative program between JAERI and universities using plasma facing materials in JT-60U

N. Miya [a,*], T. Tanabe [b], M. Nishikawa [c], K. Okuno [d], Y. Hirohata [e], Y. Oya [f]

[a] Department of Fusion Facilities, JT-60 Facilities Division II, Naka Fusion Research Establishment, Japan Atomic Energy Research Institute, Mukouyama, Naka-machi, Naka-gun, Ibaraki-ken 311-0193, Japan
[b] Nagoya University, Nagoya 464-8603, Japan
[c] Kyushu University, Fukuoka 812-8581, Japan
[d] Shizuoka University, Ohya, Shizuoka 422-8529, Japan
[e] Hokkaido University, Kita-13, Nishi-8, Kita-ku, Sapporo 060-8628, Japan
[f] The University of Tokyo, Yayoi, Bunkyo-ku, Tokyo 113-0032, Japan

**Abstract**

The cooperative research program between JAERI and universities using the first wall tiles was initiated in 2001 to elucidate the plasma–wall interactions in JT-60U. Various studies have been intensively performed from 2001 to 2002. Major research results obtained in these years were reviewed. Main topics are as follows: (1) Tritium areal distribution on plasma facing graphite tiles was measured by using tritium imaging plate technique and a combustion method. the results were compared to the simulation results for triton orbits, (2) erosion depth and deposition thickness were measured poloidally by using dial gauge and SEM on a set of W-shaped divertor tiles, (3) distribution of hydrogen isotopes and the chemical status of carbon in the divertor region were evaluated by SIMS and XPS, (4) release behavior of tritium from graphite tile samples was studied using thermal desorption, and (5) tritium degassing characteristics in tokamak exhaust were investigated by cleaning discharges.


## 1. Introduction

Understanding of plasma–wall interaction in the presently operated fusion experimental devices is crucial for a future nuclear fusion reactor design such as ITER reactor [1]. Evaluation of retention and degassing properties of tritium and deuterium in the plasma facing materials (PFM) becomes a very important issue from the viewpoint of safety for a fusion reactor. Especially, tritium inventory inside the vacuum vessel is one of the critical problems in the reactor with carbon-based material because the reactor operation may be restricted by the tritium accumulated in the carbon tiles [2]. On the other hand, studies in erosion/re-deposition on the walls of fusion experimental devices are also indispensable for the understanding of impurities transport and accumulation, hydrogen isotope migration and its accumulative inventory in the vacuum vessel, as well as for the lifetime of the divertor target [3].

For a systematic approach to above issues, a cooperative research program between JAERI and universities using the PFM of JT-60U have begun in 2001. After some preparations for the licensing of tritium use based on radiation protection regulations, a new analysis room was built in the JT-60 facility. The room is available for the surface analysis study of the PFM removed from the vacuum vessel after DD discharges in JT-60U. Arrangement of analytical instruments has been made, such as secondary ion mass spectroscopy (SIMS), X-ray photo-electron spectroscopy (XPS), and scanning electron microscope (SEM), etc. Under the cooperative program, various studies on the PFM have been performed in coordination with each particular research

* Corresponding author. Tel.: +81-29 270 7430; fax: +81-29 270 7449.
*E-mail address:* miya@naka.jaeri.go.jp (N. Miya).

0022-3115/$ - see front matter © 2004 Elsevier B.V. All rights reserved.
doi:10.1016/j.jnucmat.2004.04.219

specialties of participated universities or laboratories. Major results to date are (1) tritium profiling, (2) erosion and deposition profiling, (3) hydrogen isotopes profiling, (4) tritium release behavior and (5) wall conditioning techniques. This paper reviews these research activities carried out mainly from 2001 to 2002 by Nagoya University, Hokkaido University, University of Tokyo, Shizuoka University, Kyusyu University, and JAERI [9–13,16,19,20,23,24].

## 2. Experimental procedure

JT-60U is a noncircular tokamak device focusing on the demonstration of the physical feasibility of nuclear fusion reactors with a vacuum vessel of 3.4 m in major radius and 1.1 m (horizontal)/1.4 m (vertical) in minor radii. After the construction of JT-60U in 1990–1991 [4,5], deuterium experiments have begun at July 1991. In 1997, the divertor structure inside the vacuum vessel was modified from an open divertor to a W-shaped divertor with pumping to study high-performance plasmas and steady-state operation [6]. Fig. 1 shows a cross sectional view of the vacuum vessel and poloidal locations of analyzed tiles in the divertor region. Carbon fiber composite materials were applied for the divertor and the dome top tiles (CFC:CX-2002U) and a part of the baffle tiles (CFC:PCC-2S). All other area was covered with isotropic graphite tiles (IG-430U). Temperatures of the tiles located in the divertor region were monitored by AC thermocouples installed 6 mm under the tile surfaces.

During the operation periods from June 1997 to October 1998, about 4300 discharges (3600 D–D discharges) were made with the W-shaped divertor configuration with (or without) inner private flux pumping through a full toroidal inner slot. After the final deuterium plasma discharge period, 700 shots of hydrogen

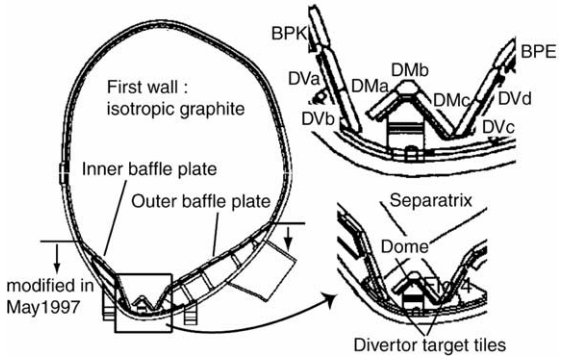


Fig. 1. Cross sectional view of the first wall and divertor regions in JT-60U with the W-shaped divertor (Inner slot pumping system); divertor tiles (DVa–d), and dome top tiles (DMa–c).

discharges were carried out to remove the surface tritium prior to the vessel vent. More than 300 shots were with neutral beam injection (NBI) heating with power of 14–23 MW. The total amount of the tritium produced during this period was 18 GBq. In December 1998, a poloidal set of divertor tiles (exposed to plasma from June 1997 to October 1998) were sampled from the #P5 section. The first wall sample tiles (exposed to plasma from March 1991 to October 1998) were also removed for the tritium measurements and surface profilometry analysis. Tritium degassing operation was executed for six operational weeks from October to December 2002. Taylor discharge cleaning (TDC), electron cyclotron resonance (ECR) discharge and glow discharge cleaning (GDC) were carried out using various working gases.

For measuring the areal distribution of tritium radioactivity a two-dimensional radiation detector, an imaging plate (IP), was applied because of its high resolution, ultrahigh sensitivity and relatively simple procedure. The IP can be used to measure the deposited tritium within a depth of about 3 μm from the surface of the sample. In the full combustion method, the tritium contained in a sample was measured by burning it in air at 1000 °C for 6 h, converting unoxidized tritium into HTO on a hot copper bed (CuO) at 500 °C. To assess the energetic triton loss from the plasma, the Orbit Following Monte-Carlo (OFMC) code [7,8] was used. Coulomb collisions between the energetic tritons and the plasma were simulated. The triton orbits was traced in the magnetic fields combined with the axisymmetric field produced by toroidal field ripple.

Erosion depths were measured directly through surface profilometry by using a dial indicator. The thickness and their microstructures of re-deposition layers were investigated by using SEM to look at sectioned specimens. The depth profiles of hydrogen and deuterium retained in graphite tiles were analyzed by SIMS by using cesium ion ($Cs^+$, 15 keV) as the primary ion with a sputtering rate of approximately 1 μm/h. The beam size was about 32 μm and the raster size was set to be $400\times400$ μm$^2$. The chemical states were studied by XPS, using a Mg-K$\alpha$ 400 W X-ray source and a hemispherical electron analyzer.

To investigate tritium release from the graphite tile a quartz reaction tube was used. A tile sample was crushed and isochronally annealed from room temperature to 1200 °C. Desorbed tritium was converted to tritiated water with a heated CuO bed and collected in two bubblers. In the tritium degassing operation, tritium concentration and chemical form were measured with an ion chamber (IC) and water bubblers. The gas species in the exhaust gas were monitored with a residual gas analyzer (RGA) system and a microgas-chromatography (MGC) [9]. Main operational conditions of ECR, TDC and GDC were as follows: (1) for ECR, toroidal magnetic field ($B_t$) of ~0.071 T, resonance frequency of

1.74, 2.0, 2.23 GHz, injection power of ~20 kW, discharge duration ($T_d$) of 1–45 min, and predicted ion injection energy ($E_{ion}$) to the wall of several 10 eV; (2) for TDC, plasma current of 50 kA, $B_t$ of ~0.73 T, $T_d$ of ~20 ms, repetition time of discharge of 1–7 s and $E_{ion}$ of several 10 eV; (3) for GDC, $T_d$ of 1/5–6 h, applied voltage of 250–600 V on four anodes, and total current of 30 A. This corresponds to current density <15 mA/cm$^{-2}$ and the mean ion flux became ~$10^{18}$ m$^{-3}$ s$^{-1}$. $E_{ion}$ was expected to several 100 eV.

## 3. Results and discussions

### 3.1. Tritium profiling [10–14]

Fig. 2 shows the surface tritium distribution of the dome top tiles in full toroidal direction by using tritium imaging plate technique (TIPT) [15]. The horizontal axis represents the position of the tiles in toroidal angle from 0° to 360°, and the vertical axis represents the tritium areal concentration of each dome top tile. The retention level clearly varied with some periodicity in the toroidal direction, the period was found to be nearly the same as the spacing of the toroidal field magnetic coils (TFMCs). This phenomenon is known as the ripple loss as described below. The toroidal magnetic field is not homogeneous because of the separated configuration of the TFMCs. Energetic ions tend to be trapped between the TFMCs where the magnetic field is weak, and then impinged onto the plasma facing walls without losing too much of their original energy. Tritons, which have 1 MeV initial energy, might behave as such energetic ions from the ripple loss.

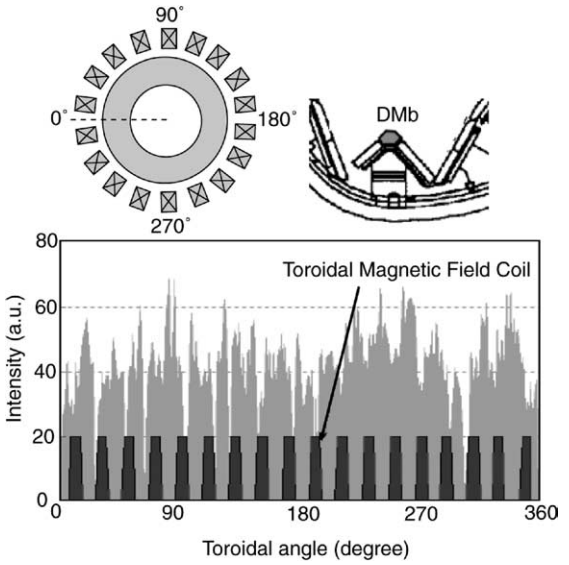


Fig. 2. Tritium distribution in toroidal direction. Tritium areal concentration of each tile is represented by gray color. Black squares represent the positions of the TMFCs. Although the distribution is comparatively homogeneous, there are some periodic waves.

Fig. 3(a) compares the IP result in the divertor region with the simulation result by using the OFMC code. In the simulation, particle flux profile was obtained for a high-$\beta$ H mode plasma discharge with high neutron yield. The IP intensity had its maximum level at the dome top tiles while it is lower in the inner and outer divertor plates. The higher levels were also observed at

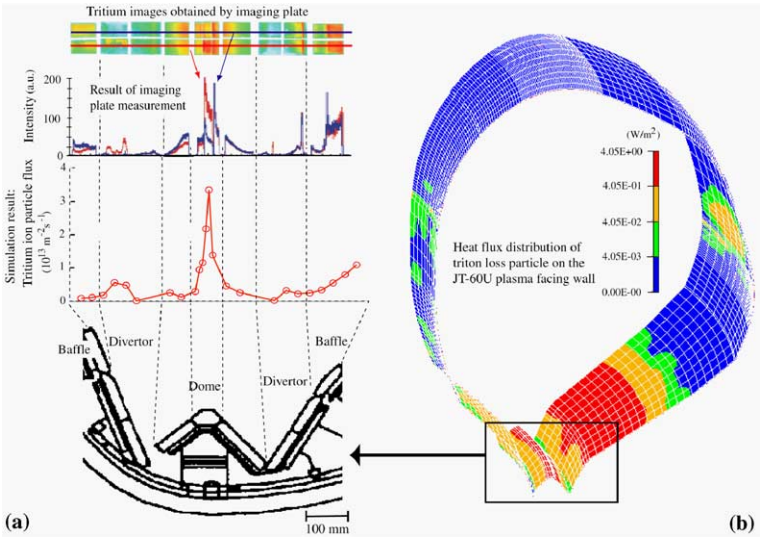


Fig. 3. The result of a comparison between the results of IP and the triton orbit following simulation in the poloidal direction (a) and the simulation of heat flux distribution (b). The triton particle fluxes by the simulation shows averaged values in the toroidal direction.

an outer baffle tile. Both results show good agreement for the tritium deposition profile. Fig. 3(b) shows a simulation result of a heat flux distribution of triton on the first wall (1/18 portion of the vessel segment under the TFMCs). In addition to the dome top and the outer baffle tiles, higher heat flux was also observed in the outer midplane region. In the toroidal direction, the heat flux was relatively high at the center of between the TFMCs. These heat fluxes show poloidal and toroidal distributions of the tritons due to the ripple loss.

In the full combustion analyses, results were consistent with those of IP and OFMC code. The highest tritium concentration of 60 kBq/cm$^3$ was found at the dome top tile. In the inner and outer divertor they were at lower levels of about 2 kBq/cm$^3$ and 250 Bq/cm$^3$, respectively. According to the OFMC results, 31% of the produced tritons ($6.5\times10^{14}$ s$^{-1}$) was lost from the plasma and implanted deeply into the wall surfaces while keeping it's initial high energy.

### 3.2. Erosion and re-deposition profiles in the divertor region [16]

Fig. 4 shows poloidal distribution of the re-deposition layer thickness and erosion depth on the W-shaped divertor tiles. The net erosion depths on the tiles were estimated from the difference between effective tile-thickness changes measured by dial indicator and re-deposition layer thickness from SEM observations. Re-deposition was predominantly found on the inner divertor plate (in DVa–b in Fig. 1) with the thickness of

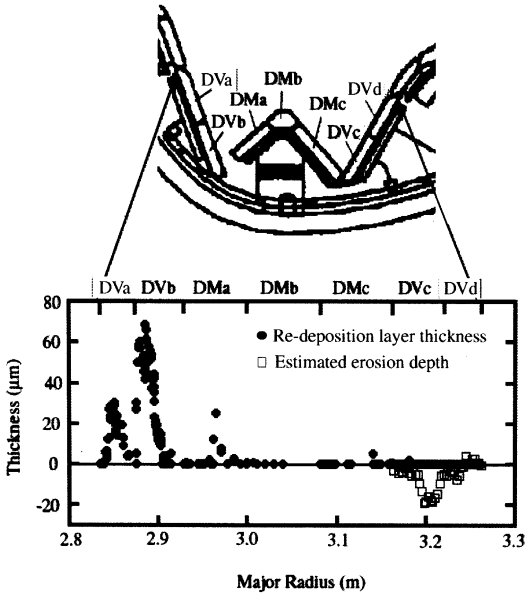


Fig. 4. Poloidal distribution of re-deposition layer thickness and erosion depth on the W-shaped divertor tiles.

up to few tens of microns, while the erosion dominated on the outer divertor plate (in DVc–d) with a maximum depth of about 20 μm. In the dome region, no continuous re-deposition layers were found on the dome top nor on the outer dome wing. Thus, significant asymmetry in the erosion/re-deposition profile was observed. From the results shown in Fig. 4, it is revealed that there is no correlation between re-deposition layers and the aforementioned tritium retention profile.

Poloidal profiles of the erosion depth and re-deposition on the inner and outer divertor targets were correlated well with integrated impinging frequency profiles of the separatrixes. The re-deposition found on the inner divertor plate was ascribed to the higher particle fluxes with the lower energies at the inner strike point, while the erosion mainly found on the outer divertor plate was ascribed to the higher heat fluxes around the outer strike points. Maximum surface temperature of the outer divertor target during shots is estimated to be in the 600–1200 K range (Fig. 7) [13]. Under such condition, the observed erosion of the outer divertor target is very probably due to chemical sputtering [17]. On the other hand, the re-deposition layer becomes dominant in the inner divertor plate due to the higher particle-recycling rate [18] and the lower temperature leads to lower erosion rate.

Fig. 5 shows SEM images of re-deposition layers at poloidal sections of the lower tile (DVb in Fig. 1). In the right-hand image, total of 60 μm deposition layers, nearly 30 μm of dense and lamellar over-layers above 30 μm of porous columnar layers, were observed in the maximum re-deposition area. The lamellar structures were sometimes observed in the deeper zones of the layers over the columnar structures. The appearance of the lamellar structures on the porous columnar layers indicates that the surface was subjected to elevated temperatures due to the lower thermal conductivity of the underneath columnar structure layers. XPS analysis showed the codeposition of 3–4 at.% B and 0.3–0.6 at.% O, Fe, Ni, Cr with carbon.

### 3.3. Surface analysis of divertor tiles by SIMS and XPS [19,20]

The depth profiles of hydrogen and deuterium retained in the graphite tiles in the divertor region were investigated by SIMS. The signal intensities of hydrogen isotopes were normalized by that of $^{12}$C. Fig. 6 shows the depth profiles of H/$^{12}$C, D/$^{12}$C and (H + D)/$^{12}$C signal intensity ratios in the dome top tile (DMb in Fig. 1). The maximum sputtering time was 6000 s, which corresponds to the depth of 1.7 μm. It was found that the ratio of H/$^{12}$C was the highest on the surface of the tile and sharply decreased with the depth and accompanying long tail. On the other hand, D/$^{12}$C first increased with depth and reached a maximum a little deeper than that

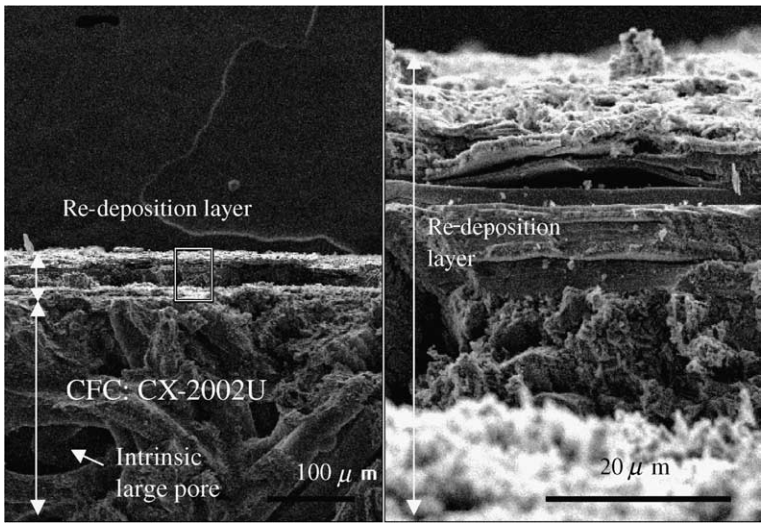


Fig. 5. SEM images at poloidal section of surface layers on the lower tile of the inner divertor (DVb). Right-hand side image is the enlargement of one enclosed with squares on the left image.

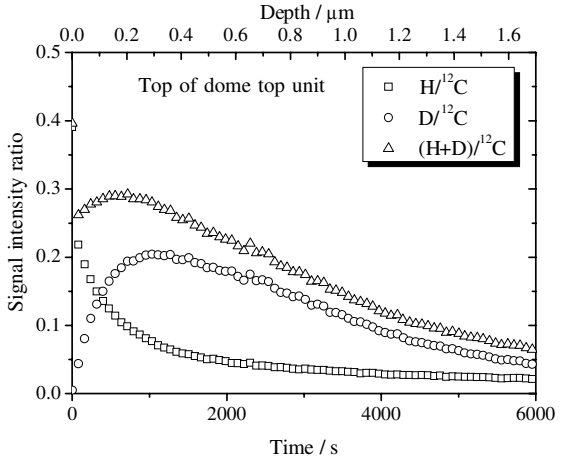


Fig. 6. Depth profiles of the signal intensity ratios of $D/^{12}C$, $H/^{12}C$ and $(H+D)/^{12}C$ in the graphite tile of the dome top unit (DMb).

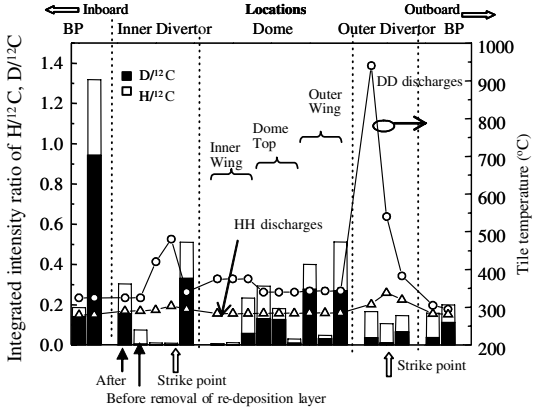


Fig. 7. Integrated intensity ratios of $D/^{12}C$ and $H/^{12}C$ of all measured sample tiles. The maximum temperature rise was monitored by thermocouples during deuterium discharges (circle) and the average temperature during hydrogen discharges (triangle) are also plotted.

of $H/^{12}C$. These results indicate that the deuterium in near surface region was replaced by hydrogen. This might to be due to the exposure to the hydrogen plasma and the deposition of H containing layers during the clean-up stage after the D–D operation, and subsequent water adsorption when exposed to air during vent.

Fig. 7 shows the retention of deuterium and hydrogen of the divertor tiles represented by integration of $\sum D/^{12}C$ and $\sum H/^{12}C$ and the temperature of each tile measured by the thermocouples. Symmetries in erosion/re-deposition strongly affects $\sum(H+D)/^{12}C$ values. $\sum H/^{12}C$ and $\sum D/^{12}C$ of the samples in the inner divertor with the re-deposition layers were considerably smaller than that of the samples in the outer divertor without the re-deposition layers. The $\sum D/^{12}C$ value after the removal of the re-deposition layer was around 0.2, approximately 70 times larger than that for the re-deposited layers indicating small hydrogen and deuterium retention in the re-deposition layer. As already suggested that thermal contact of the re-deposition layers to the tile surface may be so poor as observed in the porous columnar structure in SEM, the surface temperatures of the re-deposition layers have become higher than that measured by the thermocouples, resulting in the small $H/^{12}C$ and $D/^{12}C$ ratios in the deposited layers. In the outer divertor tiles, the small

$\sum D/^{12}C$ value was also observed at the strike point. In the case of the dome tiles and the baffle plates, the $\sum(H+D)/^{12}C$ were very large. In the dome tiles including the inner and outer wing tiles, the $\sum D/^{12}C$ and the $\sum H/^{12}C$ were largely different among the analyzed positions.

### 3.4. Tritium release behavior of tritium from graphite tiles

Tritium is isotopically exchangeable with some hydrogen existing in chemical groups such as –C–H bases or –C–OH bases that are strongly connected with the graphite surface [21]. Small part of tritium trapped in these chemical groups can remain on the surface even after being purged with a dry gas at elevated temperature. In this study, a small sample was cut from the dome unit tile of the divertor region and heated in dry inert gas and then purged with gaseous hydrogen or water vapor for tritium removal from the surface. Moreover, tritium depth profile in the graphite grain was estimated by a numerical simulation.

The sample was further cut into small pieces and crushed into granules and then packed in a quartz reaction tube. They were stepwise heated up from R.T. to 1473 K as dry argon gas was passed through the sample bed. After a small amount of released tritium was observed at 1473 K, 5000 ppm $H_2$/Ar gas or 10 000 ppm $H_2O$/Ar gas was introduced into the sample bed to remove the residual tritium from the grain surface.

Fig. 8 shows an example of tritium release curve obtained by the thermal desorption and subsequent hydrogen and water vapor purge. The amount of tritium removed by the thermal desorption reached approximately 60% of the total tritium. The residual tritium, 40% of the total, can be removed by using the isotope exchange reaction. It is confirmed that a significant amount of tritium is trapped on the grain surface and that isotope exchange reaction is required to remove all the tritium from the surface.

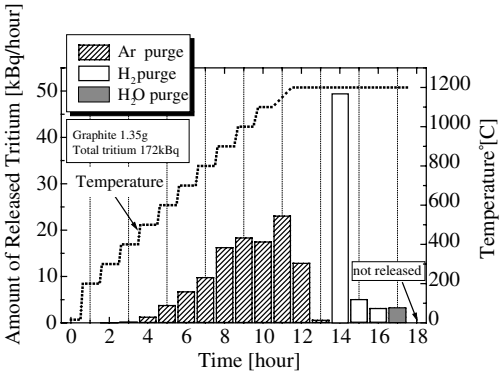


Fig. 8. Amount of tritium released from graphite sample located at dome top tile (DMb).

The release behavior of tritium was simulated using the one-dimensional diffusion equation with a diffusion coefficient of $\sqrt{1/3} \times 7.09 \times 10^{-12} \exp[-102\ (\mathrm{kJ/mol})/RT]\ \mathrm{m^2/s}$ [22]. Here, the factor $\sqrt{1/3}$ is decided by assuming the effect from isotopic ratio. Comparing the experimental results in the time dependence of tritium release with the simulation results, it can be implied that the tritium existed in the range of a few microns from the surface.

### 3.5. Tritium removal by wall conditioning discharges [23,24]

In order to establish an efficient technique for tritium removal from the vacuum vessel in JT-60U, tritium degassing operations using wall conditioning discharges of TDC, ECR and GDC were carried out for six operational weeks. Working gases were basically used in the sequence of He, Ar and $H_2$ in a week. The operations of TDC, ECR and GDC were also applied in this order. The temperature of the vacuum vessel was room temperature (RT) in the 1st, 2nd and 6th week, and 150 °C in the 3rd week, 250 °C in the 4th week and 300 °C in the 5th week.

In the case of $H_2$ gas, the removal rate was large compared with the case of noble gas (He or Ar). Here, the removal rate is defined as the total amount of removed tritium over the discharge duration. Hydrogen was most effective in tritium removal among $H_2$, He and Ar gases, and this can be attributed to chemical reactions such as isotope exchange. Effectiveness of the tritium removal was larger in GDC than in ECR and TDC. It may be explained that ion bombardment is effective in tritium removal because ion incident energy is higher in GDC than the others. The duration effect of wall conditioning discharges was confirmed by comparing the removal rate from glow discharge in the 6th week with the one in the 2nd week. The rate was reduced to ~1/4 in $H_2$ gas case, and ~1/2 in noble gas case.

The chemical form of tritium removed from the vessel was examined by three water bubblers at the wall temperature from 150 to 300 °C. The amount of tritium in water form was quite small (<1%), and the removed tritium was mainly in elemental form (HT and DT). The total amount of removed tritium was ~73 MBq. However, it was much smaller than the predicted amount of tritium (about several hundreds GBq) retained in the first wall. Most of the tritium exists deeply (~μm) in the carbon tiles, and wall conditioning discharges can only remove the tritium existing on the wall surfaces.

## 4. Conclusion

Main results in the cooperative research program between JAERI and universities are summarized as follows: (1) *Tritium profiling*, the highest tritium level

was observed at the dome top tiles in the private region, while the level was the lowest in the divertor target region. A comparison of the IP results with the simulation by OFMC code showed the tritium deposition profile was originated from the triton ripple loss; (2) *erosion and deposition profiling*, re-deposition was predominantly found on the inner divertor plate, which was ascribed to the higher particle fluxes with lower energies at the inner strike point, while the erosion mainly found on the outer divertor plate was ascribed to the higher heat fluxes around the outer strike points. Existence of the lamellar structures inside the re-deposition layers implied the higher deposition temperatures due to the lower thermal conductivity of the layers. No correlation was observed between re-deposition layers and the tritium profile; (3) *hydrogen isotopes profiling*, deuterium in the near surface region of the tile was replaced by hydrogen fueled during clean-up discharges after the D–D operation. In the inner divertor tiles with thick re-deposition layers, the least value of integrated intensity ratio $(H + D)/^{12}C$ was obtained because of the higher temperature probably due to small thermal conductivity of the tile surface; (4) *tritium release behavior*, result of tritium release experiments with graphite granules showed that a significant amount of tritium was trapped on the grain surface and that isotopic exchange reaction is required to release all the tritium from the surface; (5) *wall conditioning discharges*, in the tritium degassing operation, the wall conditioning discharges were carried out to establish efficient technique for tritium removal. Hydrogen was the most efficient gas, and glow discharge was an effective method for the tritium removal. Chemical species of removed tritium was mainly in elemental form.

## References

[1] G. Janeshitz, J. Nucl. Mater. 290–293 (2001) 1.
[2] G. Federich et al., J. Nucl. Mater. 266–269 (1999) 14.
[3] D.G. Whyte, J.P. Coad, et al., Nucl. Fusion 39 (1999) 1025.
[4] M. Kikuchi et al., in: Proceedings of the 15th Symposium on Fusion Technology, Utrecht, Netherlands, vol. 11, 1988, p. 287.
[5] H. Ninomiya et al., Plasma Dev. Oper. 1 (1990) 43.
[6] N. Hosogane et al., in: Proceedings of the 16th International Conference on Fusion Energy, Montreal, Canada, 1996, vol. 3, 1997, p. 555.
[7] K. Tobita, K. Tani, et al., Nucl. Fusion 35 (1995) 1585.
[8] K. Tobita et al., Fusion Eng. Des. 65 (2003) 561.
[9] A. Kaminaga, T. Horikawa, H. Nakamura, et al., in: Proceedings of the IEEE/NPSS Symposium on Fusion Engineering (20TH SOFE), San Diego, CA, 14–17 October 2003.
[10] T. Tanabe, K. Miyasaka, K. Masaki, et al., Fusion Sci. Technol. 41 (2002) 877.
[11] T. Tanabe, K. Miyasaka, K. Masaki, et al., J. Nucl. Mater. 307–311 (2002) 1441.
[12] K. Sugiyama, K. Miyasaka, K. Masaki, et al., Phys. Scr. T 103 (2002) 56.
[13] K. Masaki, K. Sugiyama, T. Tanabe, et al., J. Nucl. Mater. 313–316 (2003) 514.
[14] T. Tanabe, N. Berkis, N. Miya, et al., J. Nucl. Mater. 313–316 (2003) 478.
[15] T. Tanabe, V. Phillipps, Fusion Eng. Des. 54 (2003) 147.
[16] Y. Gotoh, K. Masaki, K. Kizu, et al., J. Nucl. Mater. 313–316 (2003) 370.
[17] N. Asakura et al., J. Nucl. Mater. 290 (2001) 825.
[18] S. Higashijima et al., J. Nucl. Mater. 266–299 (1999) 1078.
[19] Y. Oya, Y. Hirohata, K. Kizu, et al., J. Nucl. Mater. 313–316 (2003) 209.
[20] Y. Hirohata, Y. Oya, K. Kodama, et al., Phys. Scr. T 103 (2002) 19.
[21] N. Nakashio, M. Nishikawa, Fus. Technol. 33 (1998) 287.
[22] M. Nishikawa et al., Fus. Technol. 28 (1995) 1233.
[23] S. Higashijima, H. Nakamura, T. Horikawa, et al., in: Proceedings of 30th EPS Conference on Controlled Fusion and Plasma Physics P2-126, 2003.
[24] H. Nakamura, S. Higashijima, K. Isobe, et al., Fusion Eng. Des. 70 (2004) 163.